Suggested topics

1. Long term trends :
    a. overplot all data
    b. Data access, and plot routines
    c. 27 days variation
2. Band definition
    a. Basic definition
    b. Evolution with activity, degradation
3. Form SEM 26-34 proxy from CDS and EIT
4. Comparison to EVE 304 suggest over-correction of EVE degradation
5. Flare response comparison (like Seth)
    a. Choose flares at various positions: Mar 7 2012
    b. Try to have as many instruments as possible
    c. Create SXR spectra for selected flares
6. Degradation and selection of components (filters, CCDs, …)
7. Support for instruments campaigns and extensions

Minutes of the working sessions

Long term comparison of the various instruments (Jones, all)

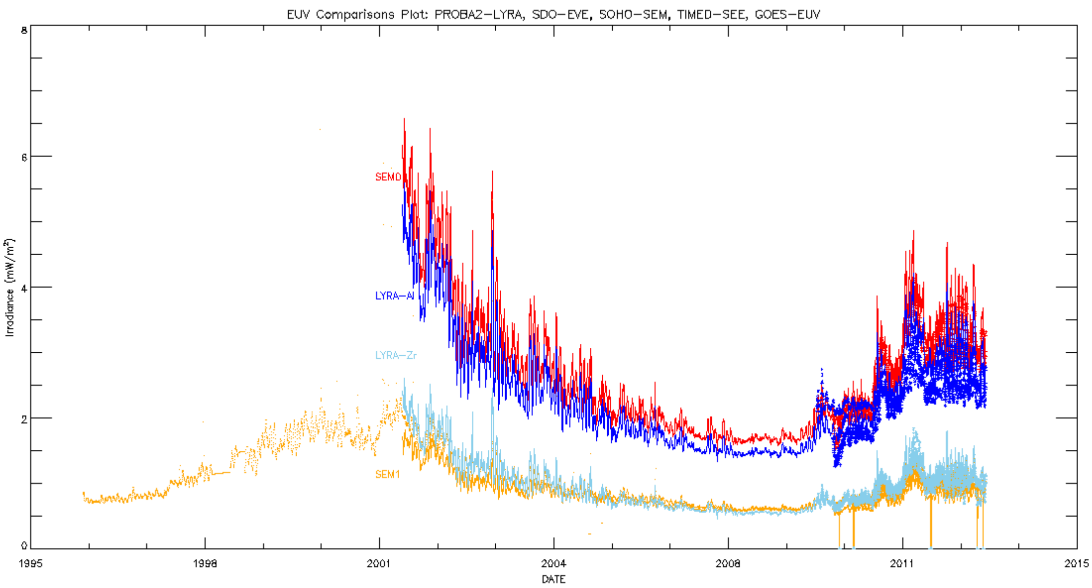

Upper curve:

- SEM (0-55 nm), with simulations from SEE and EVE
- LYRA-Al (1-80 nm), with simulations from SEE and EVE

Lower curve:

- SEM (26-34 nm), with simulations from SEE, GOES15 and EVE
- LYRA-Zr (1-20 nm), with simulations from SEE and EVE

The overall matching is quite good. When zooming in, the specific solar features like the 27-day modulation are well correlated.

Comparison of ESP-Q to SEE (Kretzschmar, Wieman)

ESP-Q (dark blue in the figure below) shows higher variability than SEE/XPS (light blue) while the pass band is similar. As a confirmation, the black curve is the SEE/XPS level 4 spectrum multiplied by the ESP-Q spectral response, and also shows much less variability.

But, ESP-Q and SEE have quite different duty cycles. It might be that the differences between ESP and XPS is at least in part caused by the fact that ESP-Q provides average daily values, and therefore includes the contribution of flare signal.

The correlation with the flare index (the red curve below), seems to validate this hypothesis.

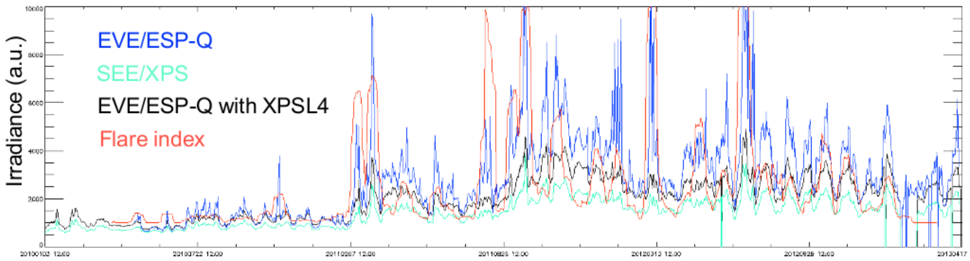

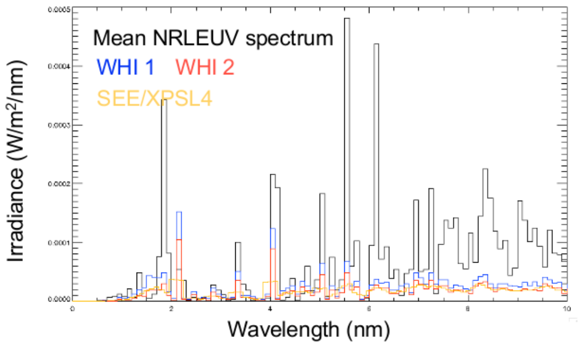

The lower panel shows the reference spectra used for the calibration of ESP-Q (blue and red), toghether with the SEE/XPS spectrum (black) used in the simulation mentioned previously. The differences between those spectra can also participate to the lesser variability of SEE.

Comparison of EVE/CDS to SEM 1st order (Del Zanna, Andretta, Wieman)

The idea is to improve the use of standard reference spectra for SEM using SDO/EVE after May 2010 and SOHO/NIS before (for a few dates).

The EVE comparison is very simple. The figure shows the predicted SEM DN/s based on the rocket EVE spectrum of 23-Mar-2011. The total predicted DN/s are 105, while the observed 92. For the conversion, the degraded response for that day as calculated by Wieman was used.

CDS/NIS observes the He II and Si XI 304 A in second order, but not the rest of the band observed by SEM, which requires modeling.
CDS/NIS irradiances have been produced (as part of the SOLID work of Del Zanna) for two dates, 30-Oct-2001 and 23-Mar-2011. DEM modelling was applied, to calculate the irradiances of all the lines in the SEM band.
The CDS spectral irradiances for several lines were calculated as described by Del Zanna & Andretta (2011) using the Del Zanna+ (2010) calibration. The DEM distribution for the solar maximum case (30-Oct-2001) is shown here:

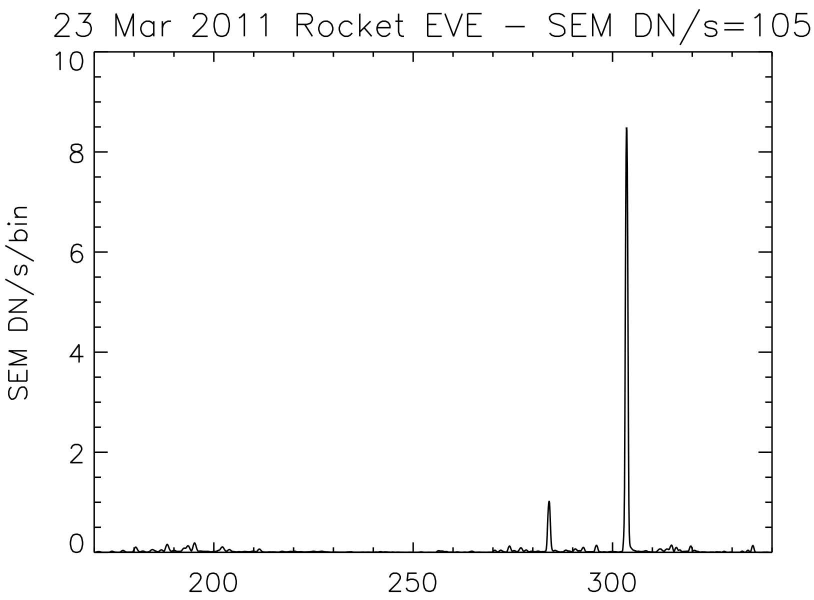

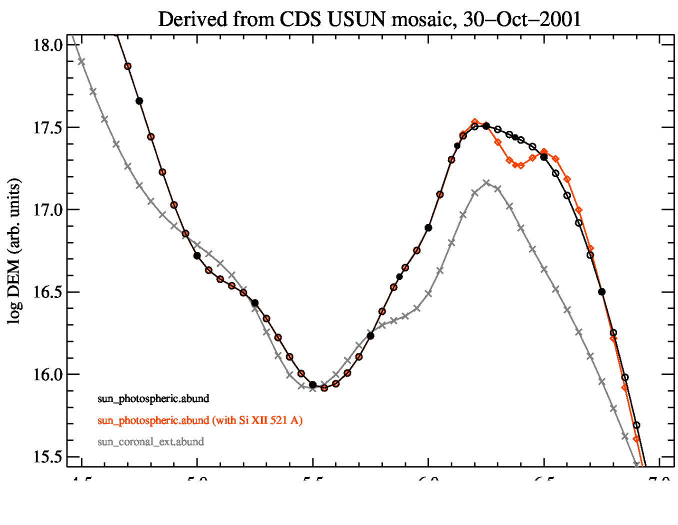

From these DEM distributions, synthetic spectra were computed with CHIANTI for the SEM 1st order bandpass. The irradiance for the strong He II 304 Å and Si XI 303 A lines were instead taken from the CDS measurements. The resulting spectra convolved with the SEM instrumental response (which included the calculated degradation for the specific dates) yielded DN/s very close to the observed ones. For the 2011 Mar 2011 we obtained exactly the same DN/s as observed by SEM, while for the 30-Oct-2001 date we obtained a value 20% lower, well below the combined uncertainties of the two instruments.

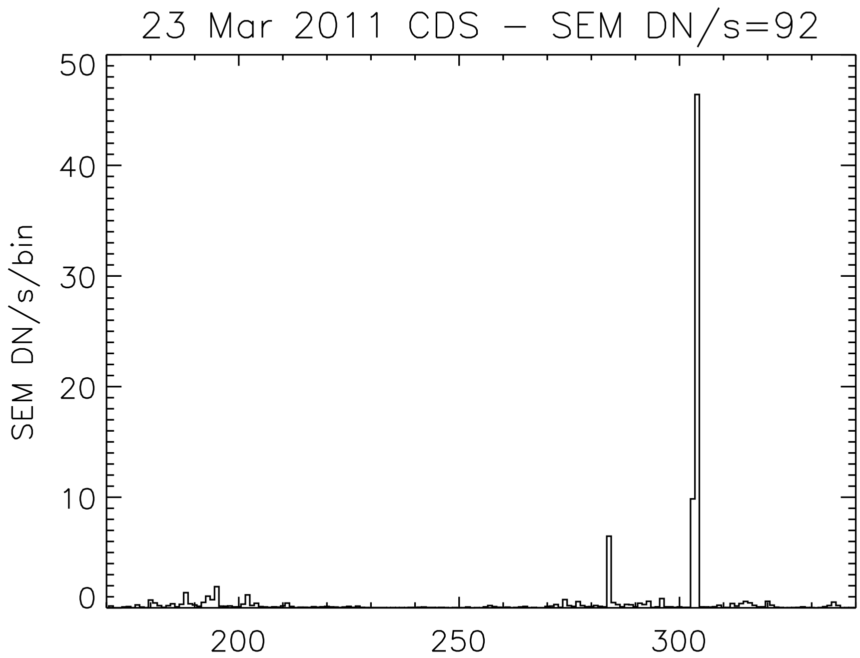

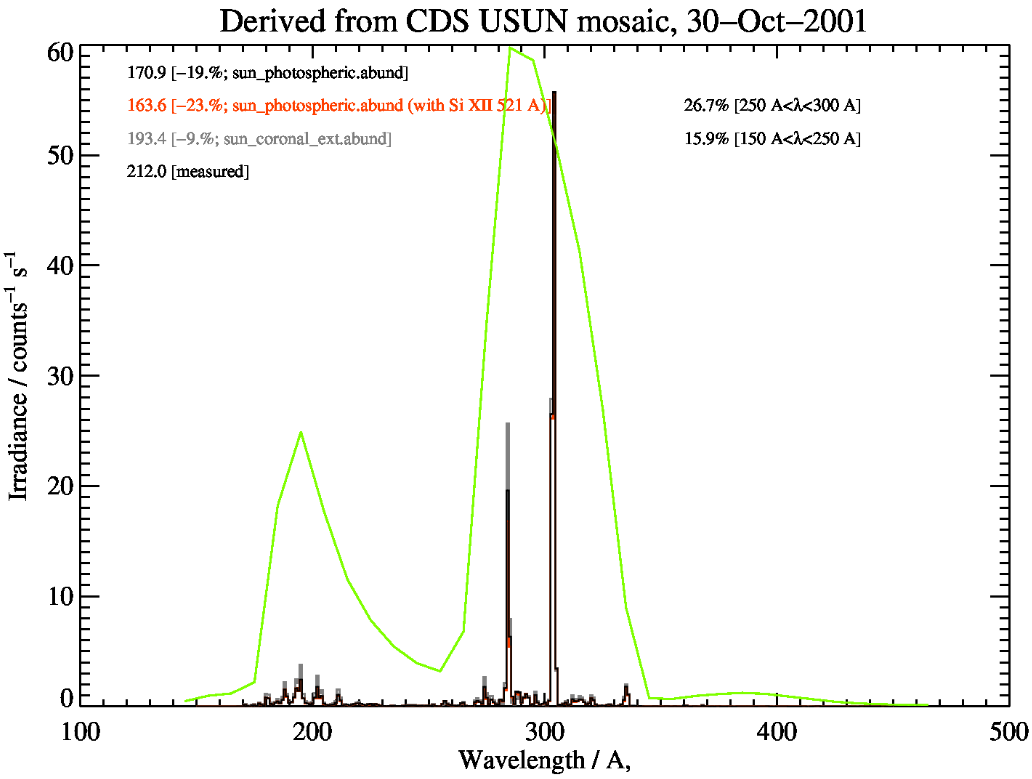

The contribution of the strong Fe XV 284 Å line to the SEM 1st order bandpass is quite significant for high solar activity, as the figure shows.

Estimation of the SXR contribution in LYRA data during flares (Del Zanna, Dominique)

The idea was to use CHIANTI to create a well-resolved SXR spectrum and attempt to determine the percentage of LYRA signal coming form the SXR during flares:

- Chosen date: X5.4 flare on March 7 2012, 00:24 – 00:27, during the peak phase; see Del Zanna & Woods (2013, A&A, in press)
- We used EVE/MEGSA spectrum (covering 6-37 nm) to establish the DEM. The strong lines from Fe XVIII-Fe XXIV constrain the DEM very well up to log T=7.3 (see plot, obtained with the Del Zanna method).

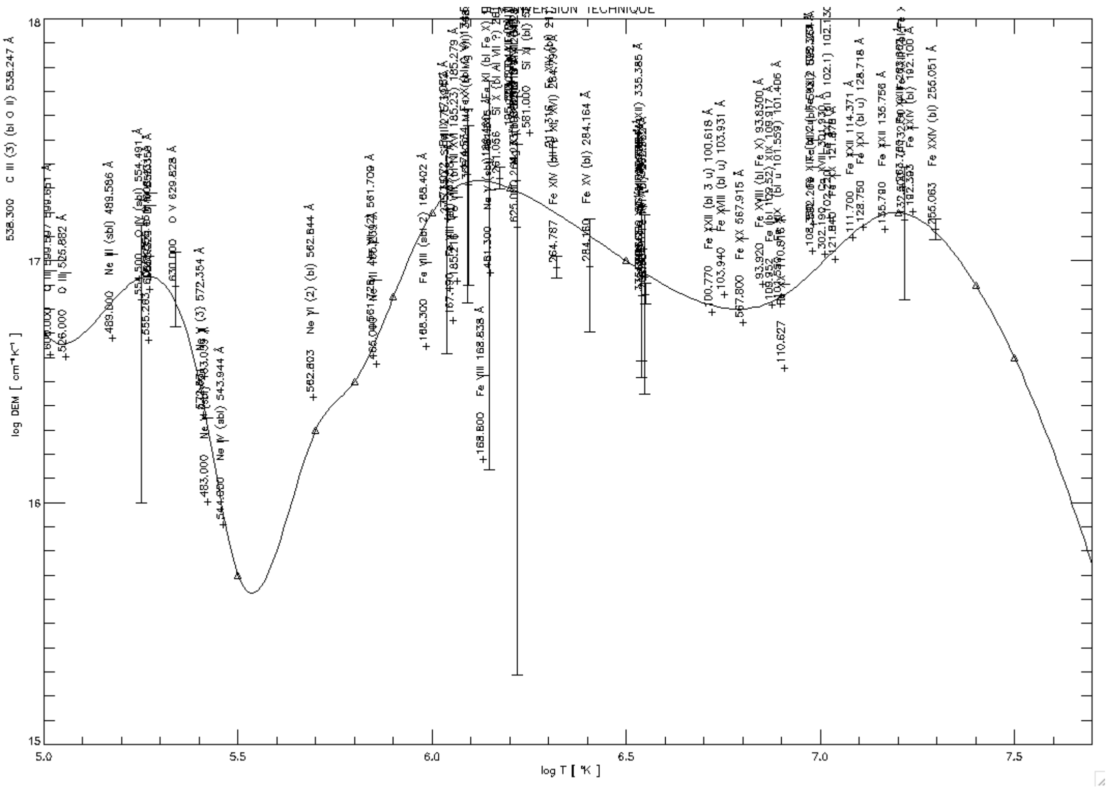

- Based on the DEM, we used CHIANTI to model the solar spectrum in SXR from 1 nm (could be down to 0.1 nm if the effective area is available for that wavelength).
- We used photospheric abundances.
- We multiplied the predicted solar spectrum by the theoretical (i.e. without taking the degradation into account) effective area of LYRA
- This allows an estimate of what comes from the various wavelengths in the SXR range (rem: in the graphs below, despite the legend, we are in counts/ms and not counts/s):
    - o LYRA aluminum channel:
      flux SXR (< 30 nm) / flux EUV = 6 (TBC?)

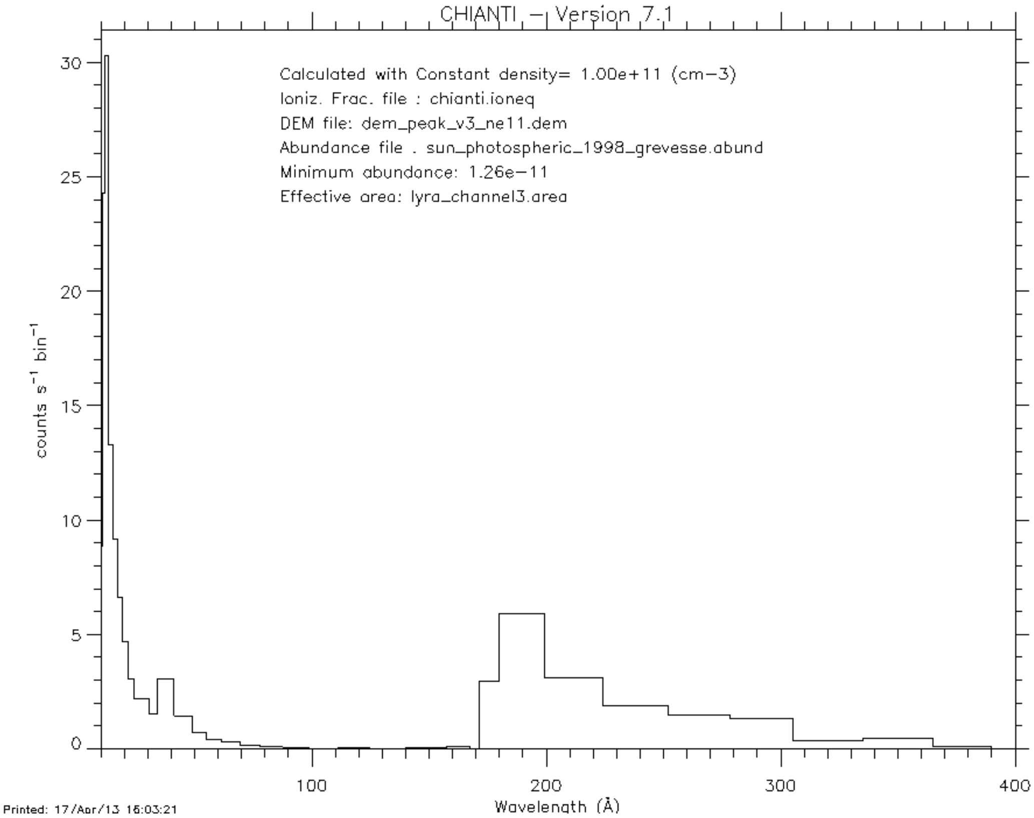

- LYRA zirconium channel:
  flux SXR (< 30 nm) / flux EUV = 30 (TBC)

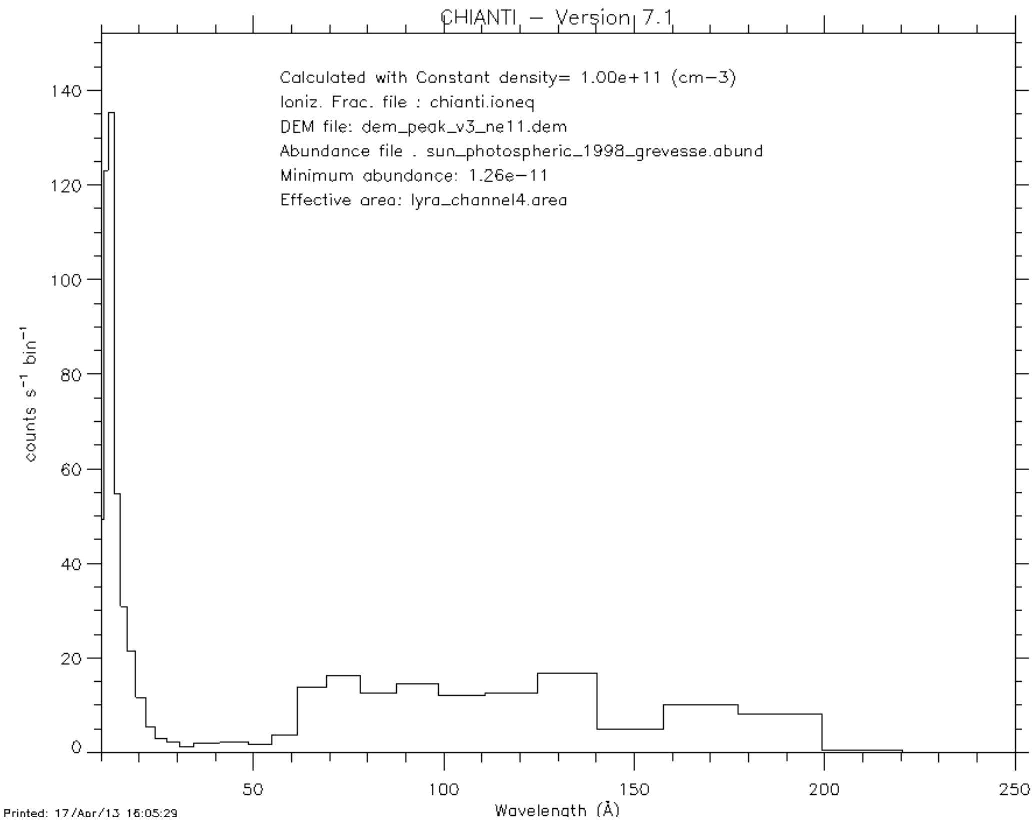

Notes:
- When comparing a flare acquisition with ESP 0-7 nm to LYRA-Zr and –Al, the latter clearly peak after, indicating some EUV remaining in LYRA channels.
- This analysis could be repeated to various dates to see the evolution of the SXR response and to other instruments

Redefinition of LYRA bandpasses

We used the reference quiet-sun WHI 2008 reference spectrum (available on http://lasp.colorado.edu/lisird/) to redefine the bandpass of LYRA lyman-alpha channel so that 95% of the measured signal effectively comes from that bandpass. To fulfill this requirement, it appears that the bandpass should be 115-220 nm. The other LYRA bandpasses are correctly defined.

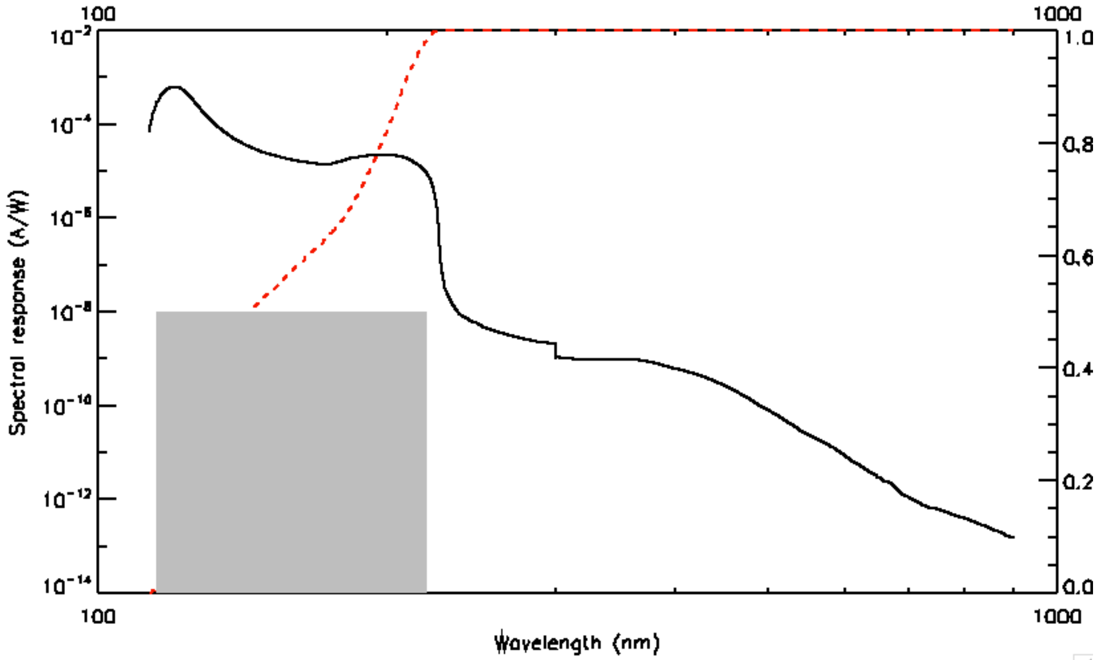

Synthesis of the optical elements used in all instruments and of the degradation they experienced

SEM Description:

Bandpasses: 26-34nm, 0.1-50nm

1. Freestanding Transmission grating, Mfr: MIT Space Nanotechnology Lab
2. Freestanding aluminum filter 150nm thick, Mfr: Luxel
3. AXUV Silicon photodiodes with 150 nm aluminum filter, Mfr: IRD

Degradation: SEM efficiency declined significantly over the first several years but has since stabilized. The loss of sensitivity is attributed to carbon buildup on the freestanding aluminum filter. The time and wavelength dependence of this degradation in the SEM flight instrument has been modeled as a time dependent buildup of carbon on the front filter surface with good results (SEM flight irradiances corrected based on this model are in good agreement with sounding rocket calibration measurements).

ESP Description:

Bandpasses: 0.1-7nm, 16.64-21.5nm, 22.28-28.78nm, 27.16-33.8nm

1. Freestanding Transmission grating, Mfr: MIT Space Nanotechnology Lab
2. Freestanding aluminum filter 150nm thick, Mfr: Luxel (three are included on the filter wheel, one primary and two redundant)
3. AXUV Silicon photodiodes with 150 nm aluminum filter, Mfr: IRD
4. Freestanding Carbon-Titanium-Carbon filter, Mfr: Luxel
5. Freestanding Aluminum-Magnesium-Aluminum filter, Mfr: Luxel

Filter degradation: ESP sensitivity is measured during daily in-flight calibrations in which the filter wheel is indexed to provide measurements with one of the redundant science filters (redundant filters are only briefly exposed during these calibrations and therefore have not suffered significant degradation). Count rates from these calibration measurements are compared to those made using the primary filter to assess its degradation. After 1000 days of operation, reductions in transmission (compared to first light values) are 62%, 48%, 30% respectively for the bands centered at 30, 26 and 18 nm respectively and 7% for the zeroth order 0.1-7nm band.

Detector degradation: Dark count levels and their dependence on temperature have changed (by ~10% at a given temperature), primarily for the zeroth order quad diode channels. These changes have occurred gradually for the most part, with the exception of a rapid shift in one of the channels that coincided with a particle event in March 2012. This degradation is likely related to either a decrease in the photodiode shunt resistance or a change in the offset voltage across the input of of the electrometer amplifier (P/N: AD549L).

Picard/Sodism

- filtres UV 215 nm : provenance --> Acton
- filtres UV 393 nm : provenance --> ANDOVER
- autres longueurs d'onde --> ANDOVER
- CCD : provenance E2V --> CCD 42-40

EUVS on GOES 13-15

Bandpasses: A: 5-15 nm, B: 25-34 nm, C: 17-67 nm, D: 17-84 nm, E: 118-127 nm

1. EUVS (3 spectrograph units: one for A and B, one for C and D (or A' and B' on GOES-14), and one for E.), Mfr: ATC
2. AXUV silicon photodiodes, Mfr: IRD
3. Gratings, (A,B: 5000 lines/mm, C,D: 2500 lines/mm, E: 1667 lines/mm), Mfr: MIT

4. Thin film filters on detectors (A: 50/200/70 nm of Ti/Mo/C, B: 150/5 nm of Al/Al2O3, C: 150/2 nm of Al/Al2O3, D: 150/2 nm of Al/Al2O3), Mfr: Lebow
5. Free standing Lyman-α filter, Mfr: Acton Labs

Degradation: Minimal/none on channels A-D. Approximately 7%/year on GOES-15 Channel E. More likely due to a contamination layer than radiation based on initial comparison with GOES 14 Channel E which was pointed away from the Sun for about a year. More work needed.

According to Viereck et al. (2007), several design features and manufacturing techniques were incorporated to minimize the impact of contamination. The first optical component is the transmission grating. The buildup of contaminants from outside the sensor will occur primarily on the grating bars which will have minimal impact on the transmission properties. The grating can accumulate 10's of nm of molecular contaminants before experiencing a noticeable change in transmission whereas an optical component such as a filter or window will exhibit a significant decrease in performance (depending on the material) for more than about 0.5 nm of contaminants. To minimize the contaminants on internal optical surfaces, the EUVS was manufactured in a clean environment. The few electronic components and wires required to control and read the silicon diodes are at the back of the optical housing and are kept extremely clean. The entire package was stored with a dry nitrogen purge or in a vacuum during most of its testing and prelaunch storage activities. Zeolite absorbers inside the optical housing are designed to capture any residual contaminants that remain inside the optical housing after launch.

GOES XRS

Bandpasses: 0.5-4 Å, 1-8Å

1. Two gas-filled ion chambers, one for each band.

Degradation: Minimal/none. We plan to quantify this.

LYRA

Bandpasses: 1-20nm, 1-80nm, 120-123nm, 190-222nm

6. Freestanding zirconium filters, 158nm thick, Mfr: Luxel
7. Freestanding aluminum filters, 141 or 300 nm thick, Mfr: Luxel
8. Lyman-Alpha interference filters, ref: 122 XN or 122N, Mfr: Acton
9. Herbzerg interference filters, ref: 220B, Mfr: Acton
10. AXUV Silicon photodiodes, Mfr: IRD
11. PIN diamond detectors, Mfr: IMO-IMOMEC
12. MSM diamond detectors, Mfr: IMO-IMOMEC

Very strong degradation mostly due to a contaminant layer (probably rtv) deposited on the filters

Perspectives

The work initiated during these working sessions has to be continued. We expect that a few papers can result from it:

- Action: Frederic to provide Peter with spatial and temporal dependences of solar EUV emission
- Comparison of SEM data to reconstructions based on CDS and on EVE spectra (Seth is in charge)
- Comparison of LYRA data to reconstructions based on CDS and on EVE spectra (Marie+ Ingolf in charge), comparison of LYRA-Al to SOLACES-Al (with Christian)
- Extension of the flare analysis performed with LYRA data and based on a CHIANTI spectra to other dates and instruments (Giulio in charge)
- Comparison of flares in LYRA and GOES, especially in lyman-alpha (Marie, Ingolf, Janet)